



Research paper

NO photooxidation with TiO₂ photocatalysts modified with gold and platinum

M.J. Hernández Rodríguez ^{a,b,*}, E. Pulido Melián ^{a,b,*}, D. García Santiago ^{a,b}, O. González Díaz ^{a,b}, J.A. Navío ^c, J.M. Doña Rodríguez ^{a,b}

^a Grupo de Fotocatálisis y Espectroscopía Aplicada al Medioambiente (FEAM)-Unidad Asociada al CSIC por el Instituto de Ciencias de Materiales de Sevilla, Centro Instrumental Químico-Físico para el Desarrollo de Investigación Aplicada (CIDIA)-Dpto. de Química, Edificio Central del Parque Científico Tecnológico, Universidad de Las Palmas de Gran Canaria, Campus Universitario de Tafira, 35017, Las Palmas, Spain

^b Instituto de Estudios Ambientales y Recursos Naturales (i-UNAT), Universidad de Las Palmas de Gran Canaria (ULPGC), 35017, Las Palmas, Spain

^c Instituto de Ciencia de Materiales de Sevilla, Centro Mixto CSIC-Universidad de Sevilla and Dpto. de Química Inorgánica, Universidad de Sevilla, Avda. Américo Vespucio s/n, 41092, Sevilla, Spain

ARTICLE INFO

Article history:

Received 4 October 2016

Received in revised form 1 December 2016

Accepted 2 December 2016

Available online 10 December 2016

Keywords:

Photocatalysis

NO_x

TiO₂

Au

Pt

ABSTRACT

In this study, a comparative analysis is made of TiO₂ modified with Pt or Au in NO photooxidation under different radiation and humidity conditions. The metals were deposited on the TiO₂ surface using two methods, photodeposition and chemical reduction. All catalysts were supported on borosilicate 3.3 plates using a dip-coating technique. These modified photocatalysts were characterized by X-ray diffraction analysis (XRD), UV-vis diffuse reflectance spectra (DRS), Brunauer-Emmett-Teller measurements (BET), transmission electron microscopy (TEM) and X-ray photoelectron spectrum analysis (XPS). It was found from the XPS results that Pt⁰ and oxidized Pt species coexist on the samples obtained by photodeposition and chemical reduction. In the case of Au, though other oxidation states were also detected the dominant oxidation state for both catalysts is Au⁰. TEM results showed most Au-C particles are below 5 nm, whereas for Au-P the nanoparticles are slightly bigger. With UV irradiation, the Pt modified catalysts do not show any significant improvement in NO photocatalytic oxidation in comparison with the unmodified P25. For Au, both modified photocatalysts (Au-P and Au-C) exceed the photocatalytic efficiency of the unmodified P25, with Au-C giving slightly better results. The incorporation of metals on the TiO₂ increases its activity in the visible region.

© 2016 Elsevier B.V. All rights reserved.

1. Introduction

The presence of NO_x in the atmosphere is a major health risk for humans [1]. Though preventative measures are now in place to reduce emissions of these gases, the search for effective corrective measures continues. Heterogeneous photocatalysis is one of the processes for the removal of these gases which is gaining in popularity, with numerous previous studies in the field reporting good results [2,3]. An in-depth study of the photocatalyst to be used is important as it may present certain drawbacks that could reduce the efficiency of the process [4]. One of the main problems is the direct competition that exists between the recombination

and spatial charge separation processes of the photogenerated electron-holes. One strategy used to limit the effect of these recombination processes is the deposition of electron-acceptor species on the catalyst surface to speed up the transportation of photoexcited electrons to the outermost of these species [5]. This strategy can be facilitated through the modification of TiO₂ photocatalysts, principally using metals [6,7]. An effective transfer is thereby produced of the photogenerated electrons from the conduction band to the metal particles because the metals have a lower Fermi level than the TiO₂ [8]. Nonetheless, contradictory results have been reported in the bibliography with respect to the efficiency of the modified catalysts [9,10]. An additional benefit of the incorporation of metals on the TiO₂ surface is that activity in the visible range (400–800 nm) improves considerably in comparison to the unmodified TiO₂ [11].

While metal incorporation to enhance photocatalytic activity has been extensively studied, very few works have been published on NO_x oxidation [12]. Though some studies have been made on the incorporation of Pt and Au, no comparison has been made using the

* Corresponding authors at: Instituto de Estudios Ambientales y Recursos Naturales (i-UNAT), Universidad de Las Palmas de Gran Canaria (ULPGC), 35017, Las Palmas, Spain.

E-mail addresses: marijosehr2@gmail.com (M.J. Hernández Rodríguez), elisendapm80@hotmail.com (E. Pulido Melián).

same deposition methodology to determine which catalyst is the most efficient. Huang et al. [13] showed that TiO₂ impregnation with Pt oxides enhances photocatalytic activity, principally in the visible range, as a consequence of the synergy of Pt oxidation states (2+ and 4+). The presence of the metal also increases the conversion rate of NO₂ to NO₃⁻. Wu et al. [14], for their part and in contrast to Huang et al. [13], determined that the appearance of Ptⁿ⁺–NO bonds can inhibit oxidation of NO to NO₂ as the surface becomes less active resulting in a more rapid deactivation of the photocatalyst. Hu et al. [15] obtained a sol-gel synthesized photocatalyst doped with Pt, reporting that 0.4% of metal is sufficient to achieve high photocatalytic efficiency. Like Huang et al. [13], they concluded that the synergy of Pt oxidation states may be beneficial for the photocatalytic process. Li et al. [16,17] performed a comparative study, incorporating Pt by photodeposition and impregnation and determining that the best results were obtained with photodeposition. Song et al. [18] concluded that Pt incorporated by deposition-precipitation resulted in better photocatalytic efficiencies than by impregnation, as the former displayed lower recombination rates. It has been shown that with pH values between 6.5 and 8.5, the addition of Pt particles is greater. With respect to Au, though several studies have been performed, Hernández-Fernández et al. [19] synthesized a TiO₂-based photocatalyst with the sol-gel method, incorporating the gold during the synthesis. It was shown that the photocatalyst synthesized with 0.5% Au obtained a high oxidation rate of 150 ppm of NO, with the enhancement being attributed principally to the size of the metal particles on the photocatalyst. Hernández-Fernández et al. [20] studied the photoactivity of TiO₂ with Au incorporation following the deposition-precipitation with urea method, obtaining degradation rates of 150 ppm of NO of above 96% with 0.3% of Au. Herranz et al. [21] performed an adsorption study of NO and O₂ onto Au particles of different diameters (2–5 nm) dispersed over TiO₂ and SiO₂, demonstrating the importance of a lower size of particle for the NO adsorption process. The improvement observed with a lower particle size was attributed to the NO being adsorbed only on the TiO₂ and, probably, on the edges of the metal nanoparticles, which are proportionally more abundant in small particles.

Taking into account the studies previously undertaken in this field and with a view to determining the most efficient metal for use in NO oxidation, the present work will consider a comparative analysis of TiO₂ modified with Pt and Au deposited using the same methodology. The two metals will be studied when deposited by photodeposition and chemical reduction, determining their activity in the ultraviolet and visible light regions as well as the effect of humidity.

2. Experimental

2.1. Synthesis of photocatalysts

The catalysts modified with Au and Pt were obtained through photodeposition (P) and chemical reduction (C). The TiO₂ photocatalyst used in the tests was the Evonik P25 (P25). In all modified photocatalysts, metal loading was 0.5 wt% (% with respect to photocatalyst weight). For photodeposition, the method previously described by Maicu et al. [22] and Hidalgo et al. [23] was used. Photodeposition of Pt (Pt-P) and Au (Au-P) was achieved using hexachloroplatinic (IV) acid (H₂PtCl₆) and tetrachloroauric acid (HAuCl₄) respectively as precursors. Solutions of the appropriate concentrations of metal chloride were prepared and mixed with suspensions of the TiO₂ (5 g L⁻¹ TiO₂), adding isopropanol as sacrificial electron donor (0.3 M). Photodeposition was performed by illuminating the suspensions for 6 h with a medium pressure mercury lamp (400 W) of photon flux ca. 2.6 × 10⁻⁷ Einstein s⁻¹ L⁻¹ in

the <400 nm region, while maintaining continuous nitrogen purging. The product was then recovered by filtration, and dried at 383 K overnight. For chemical reduction of the Pt (Pt-C), a modified version was employed of a method previously reported by Zhu et al. [24]. 0.5 g of P25 was dispersed in 25 mL of distilled water. 0.66 mL of H₂PtCl₆ solution (1.04 g/100 mL) was then added to this suspension, with impregnation taking place over 24 h under magnetic stirring. After impregnation, 2.5 mL of the mixed solution of NaOH (0.5 mol L⁻¹) and NaBH₄ (0.1 mol L⁻¹) was injected into the suspension under constant stirring (24 h). The Pt-C sample was collected by centrifugation, washed three times with distilled water and ethanol, and then dried in an oven at 353 K for 6 h. For incorporation of Au by chemical reduction (Au-C), the method described by Maicu et al. [22] was employed. 1 g of P25 was dispersed in an aqueous solution of sodium citrate (0.2 g/10 mL). This was then mixed with HAuCl₄ and kept in reflux for 1 h at 373 K in a nitrogen atmosphere. Au-C was then recovered by filtration and dried at 383 K overnight.

2.2. Dip coating

The catalysts were deposited onto previously washed 50 cm² borosilicate 3.3 plates with a dip-coating procedure (KSV-DC Dip-Coater). The plates were introduced into a 14 g L⁻¹ suspension of the catalyst in methanol at a rate of 500 mm min⁻¹, left in the suspension for 20 s and withdrawn at a rate of 120 mm min⁻¹. These cycles were repeated in each case until the previously studied optimum catalyst mass had been reached ($1.16 \pm 0.01 \text{ mg cm}^{-2}$) [25]. After conclusion of the depositing process, the plates were dried at 373 K for 2 h.

2.3. Analysis techniques

Analyses of the crystalline structure were performed by X-ray diffraction (XRD Bruker D8 Advance) with a source of Cu K α_1 radiation ($\lambda = 0.15406 \text{ nm}$) at 1.6 kW (40 kV, 40 mA). Samples were prepared by placing a drop of a concentrated ethanol dispersion of particles onto a single crystal silicon plate. Crystal sizes in the different phases were estimated from line broadening of the corresponding X-ray diffraction peaks by using the Scherrer equation. Anatase–rutile fractions were calculated taking into account the relative diffraction peak intensities of crystalline planes (101) and (111) of anatase and rutile, respectively. The morphology of the samples was studied by transmission electron microscopy (TEM) using a Philips CM 200 instrument operating at 200 kV and a nominal structural resolution of ~0.25 nm. BET surface area, pore volume and pore size measurements were carried out by N₂ adsorption at 77 K using a Micromeritics 2010 instrument. Diffuse Reflectance UV-vis Spectra (DRS-UV-vis) were recorded on a Varian Cary 5 spectrometer equipped with an integrating sphere using PTFE (poly-tetra-fluoroethylene) as reference to study the optoelectronic properties of the samples. Diffuse reflectance spectra were recorded and band-gaps values were calculated by the Kubelka-Munk function, according to the Tandon-Gupta method [26]. Field emission scanning electron microscopy (FESEM) images were obtained using a Hitachi S-4800 microscope in order to determine the thickness of the deposit on the plates. X-ray photoelectron spectroscopy (XPS) studies were carried out on a Leybold-Heraeus LHS-10 spectrometer, working with constant pass energy of 50 eV. The spectrometer main chamber, working at a pressure $<2 \times 10^{-9}$ Torr, is equipped with an EA-200 MCD hemispherical electron analyzer with a dual X-ray source working with Al K α ($h\nu = 1486.6 \text{ eV}$) at 120 W and 30 mA. Ti (2p_{3/2}) signal was used as internal energy reference in all the experiments. Samples were outgassed in the pre-chamber of the instrument at 150 °C up

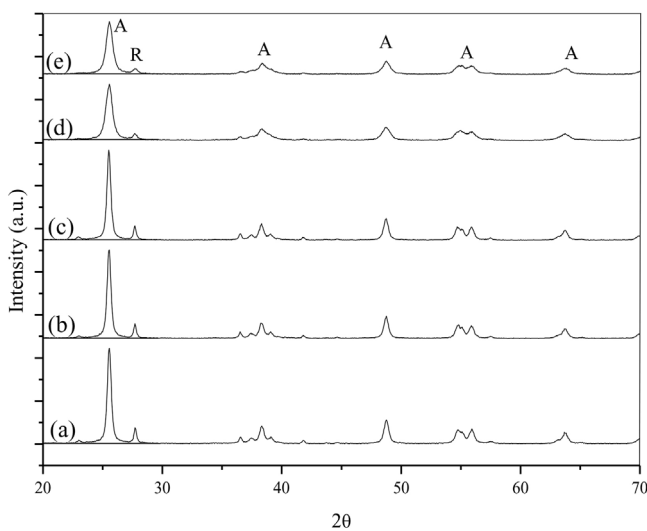


Fig. 1. XRD patterns of catalysts: P25 (a), Pt-P (b), Pt-C (c), Au-P (d), and Au-C (e).

to a pressure of $<2 \times 10^{-8}$ Torr to remove chemisorbed water. All photoelectron spectra were analyzed using Casa-XPS software.

2.4. Photoactivity study

The photoactivity tests were performed as described in previous studies [25]. The concentration of NO_x was obtained from dilution with air of a 100 ppm concentration of NO (supplied by Air Liquide) using mass flow controllers. For the addition of humidity, an extra air line was used which passed through a thermostatically controlled water bath. For the tests with visible light, a 420 nm Schott cutoff filter was placed between reactor and lamp. The operational conditions of the photoactivity tests were: 1.2 L min⁻¹, 500 ppb initial NO and 5 h of illumination. The photocatalytic results shown are the mean values of tests performed in duplicate with a maximum standard deviation of 5%. The results are expressed as percentages of degraded NO ([NO]/%) and selectivity of NO oxidation to ionic species (S):

$$[\text{NO}] / \% = \frac{[\text{NO}]_{\text{in}} - [\text{NO}]_{\text{out}}}{[\text{NO}]_{\text{in}}} \times 100 \quad (1)$$

$$S = 1 - \left(\frac{[\text{NO}_2]_{\text{out}}}{[\text{NO}]_{\text{in}} - [\text{NO}]_{\text{out}}} \right) \quad (2)$$

where $[\text{NO}]_{\text{in}}$ is the NO concentration after 30 min of adsorption or equilibrium in the dark and $[\text{NO}]_{\text{out}}$ and $[\text{NO}_2]_{\text{out}}$ are the concentrations at the end of the illumination period. All concentrations are expressed in molarities.

3. Results

3.1. Characterization of the modified catalysts

The physicochemical properties of the TiO_2 (P25) catalysts modified with 0.5 wt% of Pt and Au are shown in Table 1.

The anatase percentage does not vary between the modified photocatalysts since incorporation of the metals only takes place on the surface of the particle [27,28]. Fig. 1 shows the XRD diffraction patterns obtained for the modified catalysts, with no metal presence being observed. A metal wt% of 0.5 is a low value for detection by the measuring equipment. The TiO_2 crystalline phases present in all the catalysts are anatase (A) and rutile (R), identified by the Crystallography Open Database (COD) as COD9015929 and COD9015662, respectively. The main peak corresponding to

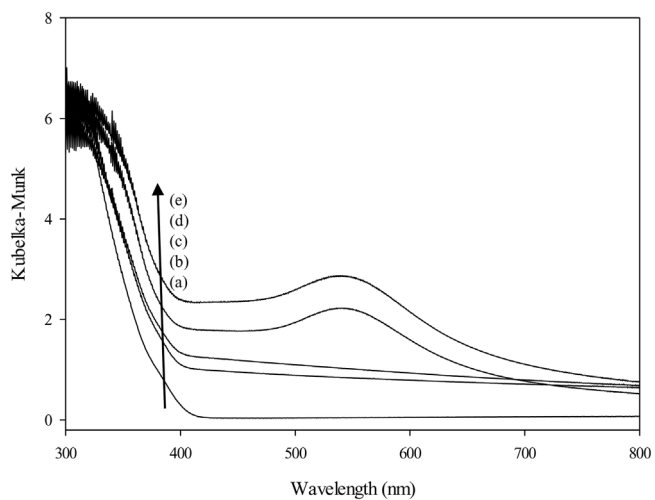


Fig. 2. DRS-UV-vis of the catalysts with P25 (a), Pt-P (b), Pt-C (c), Au-P (d), and Au-C (e).

anatase appears at approximately $2\theta = 25^\circ$ [29] and that of rutile at approximately $2\theta = 27.5^\circ$ [30]. The average crystalline sizes of anatase and rutile were obtained from XRD data with the Scherrer equation [31]. No significant variations were observed in the anatase and rutile crystal size when compared with the results for unmodified P25. This is because the modifications are not structural [32].

Fig. 2 shows the DRS-UV-vis for the photocatalysts modified with Pt and Au. Comparing the P25 spectrum with the modified samples, a similar behavior is observed with a slight shift from 400 nm to lower wavelengths ("blueshift") in the sample order Au-C > Au-P > Pt-P = Pt-C > P25. Particularly notable is that, due to the grey color they acquire, the photocatalysts with Pt show higher absorption in the visible region compared to the unmodified P25 [33]. In the Au-modified photocatalysts, a broad band appears between 500 and 620 nm with a maximum at 540 nm, which is attributed to Au surface plasmon resonance [34–36]. It has been observed by other authors that in the metal particles of Au^0 , plasmon absorption arises from the collective oscillation of free electrons of the conduction band which are induced by the incident electromagnetic radiation [37–39]. Based on the diffuse reflectance spectra and using the method described by Tandon and Gupta [26], Table 1 shows the band-gap values for the photocatalysts, with Au values lower than those for Pt, and both Au and Pt values lower than those for unmodified P25.

Table 1 shows the specific surface area and pore volume of the Pt and Au modified catalysts and of the unmodified P25. No significant variations were observed with respect to specific surface area with Pt and Au deposited on the TiO_2 surface. Some authors argue that the deposition of metal particles does not lead to any significant change in surface area [40,41]. However, an increase in the pore volume of P25 was observed, as also reported in previous works. This increase is due to the roughness resulting from the metal deposition [34,42].

The morphology of the metal particles was performed with a TEM study. Fig. 3 shows the crystals corresponding to the TiO_2 with Pt and Au surface deposited particles. The Pt deposits on the TiO_2 , for both Pt-P (Fig. 3a) and Pt-C (Fig. 3b), are spherical in shape with good dispersion and uniform distribution. In the Au micrographs, a higher dispersion can be observed of the Au-C particles (Fig. 3d) than the Au-P (Fig. 3c), with both types having spherically shaped particles.

Fig. 4 shows an estimation of the mean size distribution of the deposited Pt and Au particles observed by TEM according to the

Table 1
Main characteristics of the catalysts.

Catalysts	% Anatase	Crystal size		Surface area ($\text{m}^2 \text{ g}^{-1}$)	Band gap (eV)	Pore volumen ($\text{cm}^3 \text{ g}^{-1}$)
		Anatase (nm)	Rutile (nm)			
P25	82	20	33	48.60	3.18	0.176
Au-P	81	23	37	52.87	2.95	0.487
Au-C	81	23	34	54.76	2.81	0.474
Pt-P	82	20	33	53.80	3.04	0.352
Pt-C	82	20	32	51.52	3.07	0.399

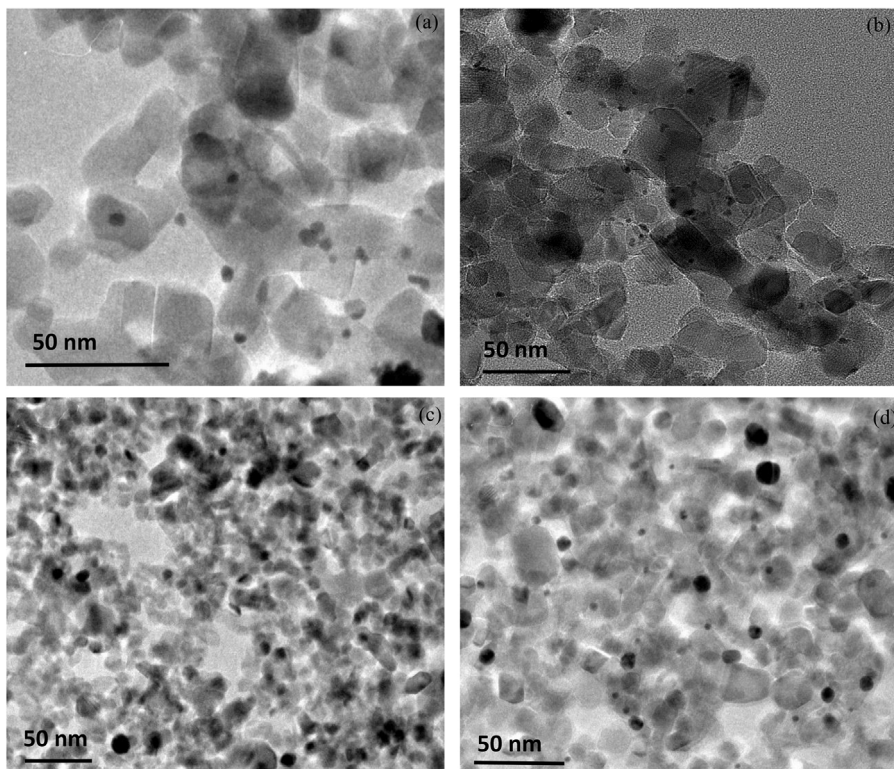


Fig. 3. TEM of Pt-P (a), Pt-C (b), Au-P (c), and Au-C (d).

modification method. For Pt, particle size distribution is similar for both photocatalysts, with most particles ranging from 2 to 5 nm and from 2 to 4 nm for Pt-P and Pt-C, respectively. For Pt-P, the diameter of the largest number of particles was between 4 and 5 nm, whereas for Pt-C the most probable mean diameter was between 3 and 4 nm. This similarity in particle distribution for Pt with different deposition methods has also been observed by other authors [15]. Greater differences are observed between the different Au deposits. There is a higher dispersal of sizes in Au-C, with nanoparticles smaller than for Au-P. Most Au-C particles are below 5 nm, whereas for Au-P the nanoparticles are slightly bigger, with most of them ranging between 6 and 9 nm.

Fig. 5 shows the XPS spectra obtained for the Pt and Au photocatalysts. Fig. 5a shows the XPS spectrum of the Ti 2p region. The signal is comprised of a doublet ($2p_{1/2}$ and $2p_{3/2}$) with a main peak binding energy of 458.3 ± 0.5 eV, corresponding to the Ti^{4+} signal of the TiO_2 [43]. A slight shift of the signals with respect to that of P25 is observed for the metal-deposited photocatalysts using the chemical reduction method. The small variations with respect to the theoretical binding energies can be explained as a result of the interactions of the metal with the titanium [44]. Fig. 5b shows that the O 1s signal is comprised of an intense peak normally attributed to the oxygen of the TiO_2 . After deconvolution, a weak shoulder is additionally observed at higher binding energies, approximately at

532 eV, attributed to oxygen present in carbonate species or surface hydroxyl ions [45]. The same signal shift is observed for the photocatalysts obtained through chemical reduction. Due to the small amount of metal contained in the samples (0.5 wt%), the peak-background ratio is low and the peaks are not clearly defined. Fig. 5c and d show the XPS spectra for the two Pt modified photocatalysts. The region Pt 4f is comprised of a doublet corresponding to the signals of the $4f_{7/2}$ and $4f_{5/2}$ peaks, which are more evident for the sample platinized by photodeposition than by chemical reduction. The binding energy of the Pt $4f_{7/2}$ for the metallic platinum Pt^0 appears at values close to 70.5 eV [46,47], while the oxidized forms ($\text{Pt}^{4+}/\text{Pt}^{2+}$) appear at binding energy values close to 75.5 eV and 72.4 eV, respectively [46]. In both the Pt-P and Pt-C samples, the Pt $4f_{7/2}$ peaks appear at values close to 70.5 eV (70.4 eV and 70.8 eV, respectively) together with the corresponding Pt $4f_{5/2}$ peaks at 74.0 eV and 73.8 eV, showing the presence of Pt^0 in both samples [48]. Additional peaks also appear at higher binding energy values, indicating the presence of $\text{Pt}^{\delta+}$ oxidized states [16,46,47]. Although it is very difficult to obtain an appropriate fit of the Pt oxidation states (+2) and (+4), the deconvolution results seem to indicate that both oxidation states could coexist in both samples. Determination of the nature of the oxidation state of the Au species (Au^0 and $\text{Au}^{\delta+}$) can be estimated from the XPS study of the Au 4f peak. The Au 4f region is characterized by a doublet corresponding to the signals

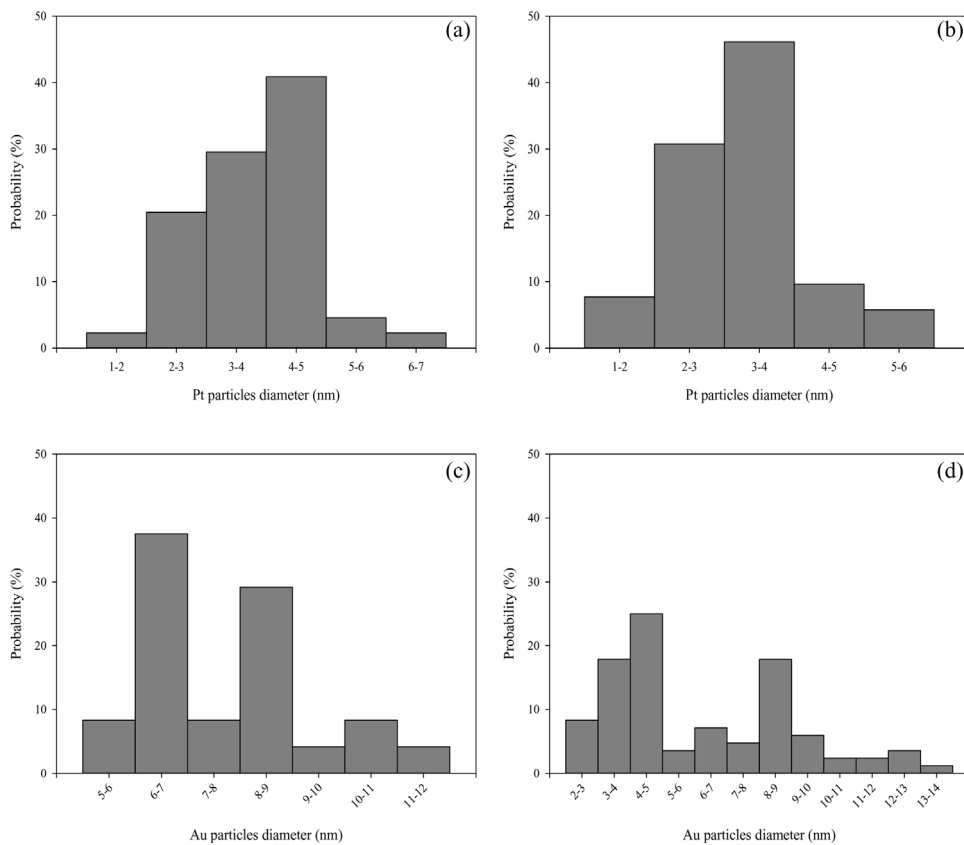


Fig. 4. Size distribution of Pt and Au particles for: Pt-P (a), Pt-C (b), Au-P (c), and Au-C (d).

of the Au $4f_{7/2}$ and Au $4f_{5/2}$ peaks with a separation of some 3.7 eV. The doublet corresponding to metallic Au (Au^0) is located at 84.0 eV ($4f_{7/2}$) and 87.5 eV ($Au 4f_{5/2}$), while the doublet of the Au oxidized states appear at higher binding energy values ($Au^+ 4f_{7/2}$ 84.7 eV and $Au^{+3} 4f_{7/2}$ 85.2 eV). By means of a deconvolution analysis, it was possible to carry out an estimation of the oxidation states of the Au in metallic state and in the oxidized states (Au^+/Au^{+3}) (Fig. 5e and f). In Au-P, the doublet corresponding to the Au^0 was detected with peaks located at 83.7 eV ($4f_{7/2}$) and 87.4 eV ($Au 4f_{5/2}$) with a difference between peaks of 3.7 eV, which are within the range of values assignable to the metallic state of Au [49–51]. These same peaks appear in Au-C, where the peaks of the doublet of the Au^0 species appear at 83.1 eV and 86.7 eV ($\Delta E \sim 3.7$ eV). In addition, in both samples, other contributions appear at higher binding energy values which could be assigned to oxidized Au states ($Au^{\delta+}$) [51]. It can be concluded that gold as Au^0 is observed with both samples and that there is evidence of less intense peaks attributable to oxidized states of the gold ($Au^{\delta+}$). The $Au^{\delta+}/Au^0$ ratio is lower in the Au-P sample.

3.2. Characterization of the plates

The deposits of $1.16 \text{ mg}\cdot\text{cm}^{-2}$ of P25 with Pt and Au, independently of the modification method, display irregular profiles, with thicknesses ranging between 0.200 and 5.520 μm (Fig. 6). No significant differences are observed if compared with the P25 deposits. Using ASTM Standard D3330/D3330M, it was determined that all deposits with Pt and Au show good adhesion (15–35%), with values similar to those for unmodified P25.

3.3. Comparison of NOx photooxidation

3.3.1. Activity under UV-irradiation

Fig. 7 shows the photoactivity of the modified catalysts, with analysis of NO oxidation and selectivity to ionic species. Reactivity was tested with different degrees of humidity. High values of NO removal were obtained with Pt-P (Fig. 7a and b) and Pt-C (Fig. 7c and d) after 5 h, with values above 80% except for Pt-P in the absence of humidity. A lack of humidity hinders NO oxidation, with Pt-P showing a sharp fall after 2.5 h and Pt-C a gentler one after 3 h. Humidity also seems to affect the Pt-P catalyst more, with the activity of this catalyst falling slightly as humidity rises. This is the most commonly observed trend in the bibliography, and is attributed to the presence of water favoring the competition of the molecules of the pollutant with those of the water for the adsorption centers of the photocatalyst [52,53]. Sleiman et al. [54] also attribute this decrease to the formation of layers of water on the TiO₂ surface, which does not allow adsorption of the molecule for its subsequent oxidation. However, the Pt-C maintains a more stable degradation percentage for all humidity levels. As for the selectivity analysis, there is a clear trend for both photocatalysts with the level of humidity; oxidation of the formed NO₂ decreases as humidity rises. The Pt-P shows a decrease in selectivity over time from the start, whereas for Pt-C the decrease, though having practically the same slope, is delayed in time, with a sort of smoothing out effect taking place except for selectivity at 65% RH which shows a very significant fall. In short, the biggest differences are found at the upper and lower humidity levels, with Pt-C performing best in the absence of humidity and Pt-P with 65% RH. These slight differences could be attributed to the differences in Pt speciation which it has not been possible to determine precisely due to the low intensity of the signal as a result of the low metal percentage. Although after 5 h of illumination both ph-

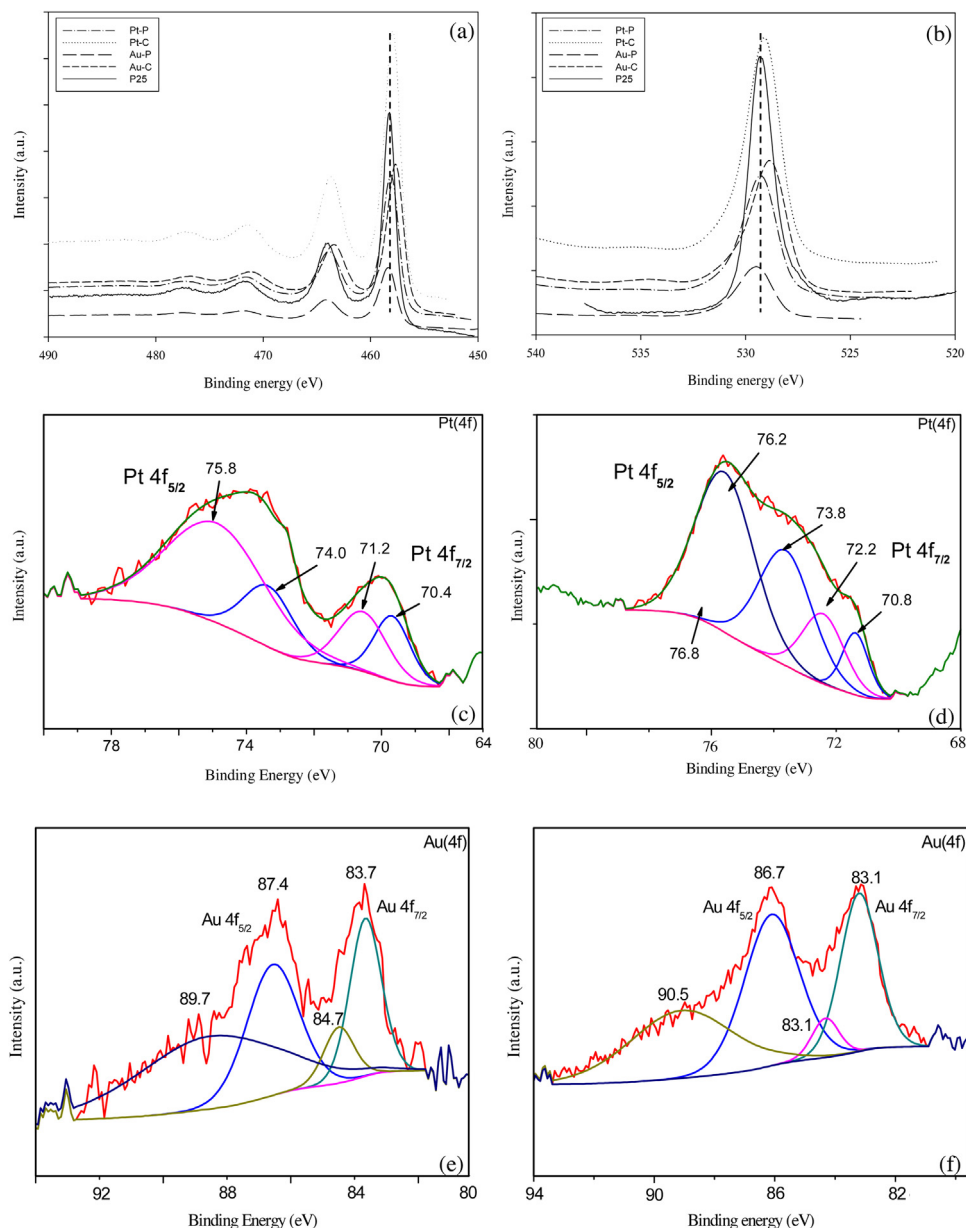


Fig. 5. XPS of samples modified with Pt and Au: (a) Ti (2p), (b) O 1s, (c) Pt (4f) of Pt-P, (d) Pt (4f) of Pt-C, (e) Au (4f) of Au-P, (f) Au (4f) of Au-C.

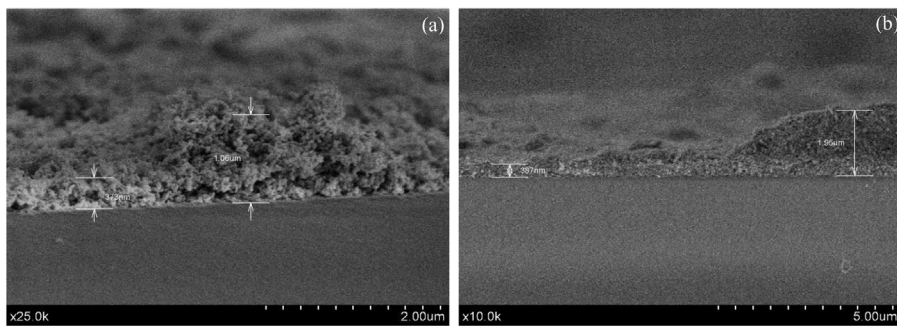


Fig. 6. Deposit of 1.16 mg cm^{-2} of P25 (a) and Au-C (b).

tocatalysts continued to show high activity, according to Wu et al. [14] an important deactivation could take place at longer illumination times. Possible reasons for deactivation include the fact that, despite the oxidized species of Pt being reduced as a result of the

effect of illumination, Pt^{2+} are formed from corrosion with HNO_3 and the Pt^{n+} -nitrosyl bonds that are produced inhibit the oxidation.

For Au-P (Fig. 7e and f) and Au-C (Fig. 7g and h), high NO oxidation percentages are obtained of over 90%, independently of the

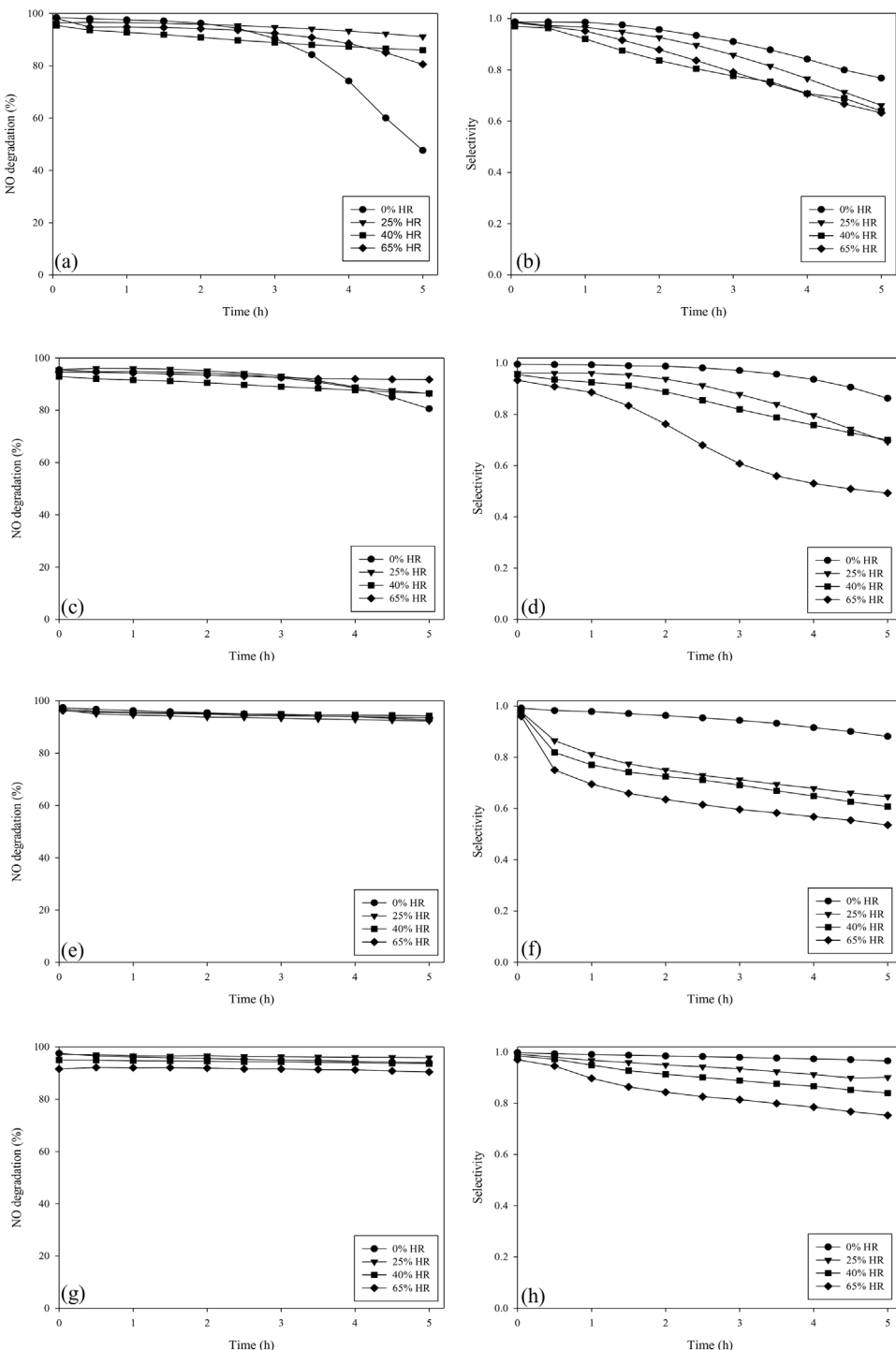


Fig. 7. Variations of NO conversion efficiency and selectivity with irradiation time for Pt-P (a)–(b), Pt-C (c)–(d), Au-P (e)–(f) and Pt-C (g)–(h) with different degrees of humidity.

humidity conditions considered. The presence of humidity does not seem to prevent photoactivity with respect to NO oxidation, with stability being maintained over the 5 h of illumination. As with the Pt, greater variations are observed in terms of selectivity. Selectivity decreases with illumination time and its values at 5 h are again lower as humidity increases due to the competition of water molecules for the active centers. A less marked decrease is observed for the catalysts obtained through chemical reduction than by photodeposition, independently of the degree of humidity. At all humidity levels, the selectivity values at 5 h for Au-C are higher than for Au-P and higher than those obtained with the

Pt catalysts. Particle size may be the most significant factor for explaining differences in photocatalytic performance of Au-P and Au-C, in addition to the slight differences showed by XPS that reveal a higher content in Au^0 for Au-C. Other authors have highlighted the importance of incorporating the Au as ultra-fine particles, particularly below 5 nm, to obtain a more efficient performance of the metal [55,56]. Kowalska et al. [57] reported that a smaller particle size leads to a more negative Fermi level, which hence allows a greater charge separation.

In terms of a comparison with the unmodified P25 (Fig. 8), the Pt modified catalysts do not show any significant improvement in NO

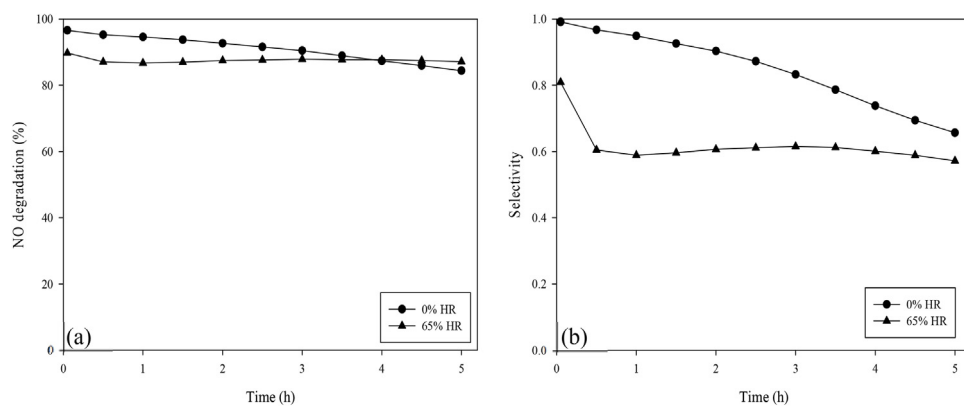


Fig. 8. Variations of NO conversion efficiency (a) and selectivity (b) with irradiation time for P25.

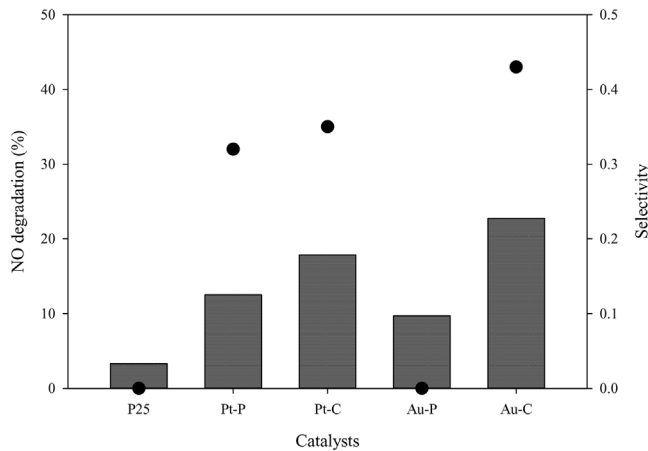


Fig. 9. Photoactivity and selectivity of photocatalysts with visible light and 65% relative humidity.

photocatalytic oxidation and in some cases the results are worse. For Au, both photocatalysts exceed the photocatalytic efficiency of the unmodified P25, with Au-C being slightly better. The enhanced photoactivity is attributed to a decrease in the recombination rate of the e^-/h^+ pairs and high interaction of the NO molecules with the photocatalyst surface [19,20,58].

3.3.2. Activity in the visible region

Fig. 9 shows NO oxidation and selectivity obtained after 5 h of illumination for the Pt and Au modified photocatalysts with 65% RH. All the modified catalysts showed an enhancement in photocatalytic efficiency compared to the unmodified P25, though in different ways. The presence of metals increases activity in the visible region where they have greater absorption and reduce recombination of the e^-/h^+ pairs [59]. The decrease in the selectivity values is due to the conversion of NO_2 to NO_3^- requiring more photon energy than the step from NO to NO_2 (44), but in general they remain above the corresponding value for the unmodified photocatalyst. Activity in the visible of both Pt-P and Pt-C was more than 300% higher than that of the unmodified P25. The enhancement of photocatalytic efficiency can be attributed to the presence of oxidized Pt species on the surface of the TiO_2 [60], and to the presence of Pt oxides. It has been shown that PtO (semiconductor with a band gap of 0.86 eV [61]) is able to photogenerate e^-/h^+ pairs when it absorbs visible light, favoring the transfer of generated e^- to the conduction band of the TiO_2 , which results in a higher flow of electrons and, therefore, a greater photocatalytic efficiency [62]. As for the Pt modified catalysts, Au-P saw a 300% increase in NO oxidation with respect to the unmodified P25, though selectivity was

unchanged, with accumulated oxidized NO remaining as NO_2 . Oxidation of NO with Au-C was 700% higher and selectivity increased it to 0.42. Activity in the visible region of the Au modified photocatalysts benefitted from the presence of plasmons when the metal was incorporated in the TiO_2 , enabling good promotion of the separation of photogenerated charges [63]. In addition, the high efficiency of Au-C was conditioned by the smaller size of the metal particles.

4. Conclusions

The incorporation of metals on the TiO_2 surface is not always beneficial in terms of enhancing photocatalytic efficiency in NO oxidation with UV light. However, the improvement is significant with visible light. For UV light, no significant increase in activity was observed after modification of P25 with Pt, whether using the photodeposition or chemical reduction method. However, both tested Au incorporation methods resulted in improved efficiencies compared to the unmodified P25 and the Pt-modified P25, independently of the degree of humidity or the applied wavelength. The oxidized Pt particles caused a bigger slowdown in oxidation for 5 h. For the Au, the chemical reduction method gave better results than the photodeposition one. Due to the small differences in the oxidation states with both methods, the morphology of the particles may well be the most significant factor, with the photocatalytic process being favored by the presence of spherical particles smaller than 5 nm. The incorporation of metals on the TiO_2 increases its activity in the visible region, displaying greater absorption in that range and decreasing recombination of the e^-/h^+ pairs. The P25 degrades the initial NO by 3.3% with visible light, whereas the Au-C degrades it by 22.8%.

Acknowledgments

We are grateful for the financial support of the Spanish Ministry of Economy and Competitiveness through the project IPT-2012-0927-420000 (HORMIFOT) and thank the Spanish Ministry of Science and Innovation for the UNPL10-3E-726 infrastructure co-financed with ERDF funds. Part of this work was supported by research funding from Project Ref. CTQ2015-64664-C2-2-P (MINECO/FEDER, EU). XPS and other research services of SITIUS University of Seville are also acknowledged. M.J. Hernández Rodríguez and E. Pulido Melián would also like to thank the University of Las Palmas de Gran Canaria for, respectively, their research training grant and postdoctoral contract.

References

- [1] J.N. Armor, Review: environmental catalysis, *Appl. Catal. B* 1 (1992) 221–256.

- [2] J. Ângelo, L. Andrade, L.M. Madeira, A. Mendez, An overview of photocatalysis phenomena applied to NO_x abatement, *J. Environ. Manage.* 129 (2013) 522–539.
- [3] J. Lasek, Y.-H. Yu, J.C.S. Wu, Removal of NO_x by photocatalytic processes, *J. Photochem. Photobiol. C* 14 (2013) 29–52.
- [4] S.W. Verbruggen, Review: TiO₂ photocatalysis for the degradation of pollutants in gas phase: from morphological design to plasmonic enhancement, *J. Photochem. Photobiol. C* 24 (2015) 64–82.
- [5] O. Carp, C.L. Huisman, A. Reller, Photoinduced reactivity of titanium dioxide, *Prog. Solid State Chem.* 32 (2004) 33–177.
- [6] G. Colón, M. Maicu, M.C. Hidalgo, J.A. Navío, A. Kubacka, M. Fernández-García, Gas phase photocatalytic oxidation of toluene using highly active Pt doped TiO₂, *J. Mol. Catal. A: Chem.* 320 (2010) 14–18.
- [7] K. Hashimoto, K. Sumida, S. Kitano, K. Yamamoto, N. Kondo, Y. Kera, H. Kominami, Photo-oxidation of nitrogen oxide over titanium (IV) oxide modified with platinum or rhodium chlorides under irradiation of visible light or UV light, *Catal. Today* 144 (2009) 37–41.
- [8] V. Etacheri, C. Di Valentini, J. Schneider, D. Bahnemann, S.C. Pillai, Review: visible-light activation of TiO₂ photocatalysts: advances in theory and experiments, *J. Photochem. Photobiol. C* 25 (2015) 1–29.
- [9] H.M. Sung-Suh, J.R. Choi, H.J. Hah, S.M. Koo, Y.C. Bae, Comparison of Ag deposition effects on the photocatalytic activity of nanoparticulate TiO₂ under visible and UV light irradiation, *J. Photochem. Photobiol. A* 163 (2004) 37–44.
- [10] A. Sclefani, J.M. Herrmann, Influence of metallic silver and of platinum-silver bimetallic deposits on the photocatalytic activity of titania (anatase and rutile) in organic and aqueous media, *J. Photochem. Photobiol. A* 113 (1998) 181–188.
- [11] M.M. Ballari, J. Carballada, R.I. Minen, F. Salvadores, H.J.H. Brouwers, O.M. Alfano, A.E. Cassano, Visible light TiO₂ photocatalysts assessment for air decontamination, *Process Saf. Environ. Prot.* 101 (2016) 124–133.
- [12] M.V. Sofianou, N. Boukos, T. Vaimakis, C. Trapalis, Decoration of TiO₂ anatase nanoplates with silver nanoparticles on the {1 0 1} crystal facets and their photocatalytic behaviour, *Appl. Catal. B* 158 (2014) 91–95.
- [13] C.H. Huang, I.-K. Wang, Y.M. Lin, Y.H. Tseng, C.M. Lu, Visible light photocatalytic degradation of nitric oxides on PtO_x-modified TiO₂ via sol-gel and impregnation method, *J. Mol. Catal. A: Chem.* 316 (2010) 163–170.
- [14] Z. Wu, Z. Sheng, Y. Liu, H. Wang, J. Mo, Deactivation mechanism of PtO_x/TiO₂ photocatalyst towards the oxidation of NO in gas phase, *J. Hazard. Mater.* 185 (2011) 1053–1058.
- [15] Y. Hu, X. Song, S. Jiang, C. Wei, Enhanced photocatalytic activity of Pt-doped TiO₂ for NO_x oxidation both under UV and visible light irradiation: a synergistic effect of lattice Pt⁴⁺ and surface PtO, *Chem. Eng. J.* 274 (2015) 102–112.
- [16] L. Li, Q. Shen, J. Cheng, Z. Hao, Catalytic oxidation of NO over TiO₂ supported platinum clusters I. Preparation, characterization and catalytic properties, *Appl. Catal. B* 93 (2010) 259–266.
- [17] L. Li, Q. Shen, J. Cheng, Z. Hao, Catalytic oxidation of NO over TiO₂ supported platinum clusters. II: mechanism study by *in situ* FTIR spectra, *Catal. Today* 158 (2010) 361–369.
- [18] S. Song, Z. Sheng, Y. Liu, H. Wang, Z. Wu, Influences of pH value in deposition-precipitation synthesis process on Pt-doped TiO₂ catalysts for photocatalytic oxidation of NO, *J. Environ. Sci.* 24 (2012) 1519–1524.
- [19] J. Hernández-Fernández, A. Aguilar-Elguezabal, S. Castillo, B. Cerón-Ceron, R.D. Arizabal, M. Moran-Pineda, Oxidation of NO in gas phase by Au-TiO₂ photocatalysts prepared by the sol-gel method, *Catal. Today* 148 (2009) 115–118.
- [20] J. Hernández-Fernández, R. Zanella, A. Aguilar-Elguezabal, R.D. Arizabal, S. Castillo, M. Moran-Pineda, Decomposition of NO in gas phase by gold nanoparticles supported on titanium dioxide synthesized by the deposition-precipitation method, *Mater. Sci. Eng. B* 174 (2010) 13–17.
- [21] T. Herranz, X. Deng, A. Cabot, Z. Liu, Miquel Salmeron, In situ XPS study of the adsorption and reactions of NO and O₂ on gold nanoparticles deposited on TiO₂ and SiO₂, *J. Catal.* 283 (2011) 119–123.
- [22] M. Maicu, Estudio de la actividad fotocatalítica de sistemas basados en TiO₂, sulfatado y no sulfatado, y modificado con Pt, Au y Pd, University of Seville, 2010, 16th February.
- [23] M.C. Hidalgo, M. Maicu, J.A. Navío, G. Colón, Study of the synergic effect of sulphate pre-treatment and platinisation on the highly improved photocatalytic activity of TiO₂, *Appl. Catal. B* 81 (2008) 49–55.
- [24] X. Zhu, B. Cheng, J. Yu, W. Ho, Halogen poisoning effect of Pt-TiO₂ for formaldehyde catalytic oxidation performance at room temperature, *Appl. Surf. Sci.* 364 (2016) 808–814.
- [25] M.J. Hernández Rodríguez, E. Pulido Melián, O. González Díaz, J. Araña, M. Macías, A. González Orive, J.M. Doña Rodríguez, Comparison of supported TiO₂ catalysts in the photocatalytic degradation of NO_x, *J. Mol. Catal. A: Chem.* 413 (2016) 56–66.
- [26] S.P. Tandon, J.P. Gupta, Measurement of forbidden energy gap of semiconductors by diffuse reflectance technique, *Physica* 38 (1) (1970) 363–367.
- [27] G. Rothenberger, J. Moser, M. Graetzel, N. Serpone, D.K. Sharma, Charge carrier trapping and recombination dynamics in small semiconductor particles, *J. Am. Chem. Soc.* 107 (1985) 8054–8059.
- [28] O. Rosseler, M.V. Shankar, M. Karkmaz-Le Du, L. Schmidlin, N. Keller, V. Keller, Solar light photocatalytic hydrogen production from water over Pt and Au/TiO₂(anatase/rutile) photocatalysts: influence of noble metal and porogen promotion, *J. Catal.* 269 (2010) 179–190.
- [29] H.G. Yang, C.H. Sun, S.Z. Qiao, J. Zou, G. Liu, S.C. Smith, H.M. Cheng, G.Q. Lu, Anatase TiO₂ single crystals with a large percentage of reactive facets, *Nature* 453 (2008) 638–641.
- [30] K. Thamaphat, P. Limsuwan, B. Ngotawornchai, Phase characterization of TiO₂ powder by XRD and TEM, *Nat. Sci.* 42 (2008) 357–361.
- [31] M. Yan, F. Chen, J. Zhang, M. Anpo, Preparation of controllable crystalline titania and study on the photocatalytic properties, *J. Phys. Chem. B* 109 (2005) 8673–8678.
- [32] J. Araña, O. González Díaz, J.M. Doña Rodríguez, J.A. Herrera Melián, C. Garriga i Cabo, J. Pérez Peña, M.C. Hidalgo, J.A. Navío-Santos, Role of Fe³⁺/Fe²⁺ as TiO₂ dopant ions in photocatalytic degradation of carboxylic acids, *J. Mol. Catal. A: Chem.* 197 (2003) 157–171.
- [33] Z. Yang, J. Lu, W. Ye, C. Yu, Y. Chang, Preparation of Pt/TiO₂ hollow nanofibers with highly visible light photocatalytic activity, *Appl. Surf. Sci.* 392 (2017) 472–480.
- [34] J.A. Ortega Méndez, C.R. López, E. Pulido Melián, O. González Díaz, J.M. Doña Rodríguez, D. Fernández Hevia, M. Macías, Production of hydrogen by water photo-splitting over commercial and synthesised Au/TiO₂ catalysts, *Appl. Catal. B* 147 (2014) 439–452.
- [35] A. Golabiewska, W. Lisowski, M. Jarek, G. Nowaczyk, A. Zielińska-Jurek, A. Zaleska, Visible light photoactivity of TiO₂ loaded with monometallic (Au or Pt) and bimetallic (Au/Pt) nanoparticles, *Appl. Surf. Sci.* 317 (2014) 1131–1142.
- [36] S. Bera, J.E. Lee, S.B. Rawal, W.I. Lee, Size-dependent plasmonic effects of Au and Au@SiO₂ nanoparticles in photocatalytic CO₂ conversion reaction of Pt/TiO₂, *Appl. Catal. B* 199 (2016) 55–63.
- [37] R. Zanella, S. Giorgio, C.H. Shin, C.R. Henry, C. Louis, Characterization and reactivity in CO oxidation of gold nanoparticles supported on TiO₂ prepared by deposition-precipitation with NaOH and urea, *J. Catal.* 222 (2004) 357–367.
- [38] P.V. Kamat, Photophysical, photochemical and photocatalytic aspects of metal nanoparticles, *J. Phys. Chem. B* 106 (2002) 7729–7744.
- [39] L.G. Devi, R. Kavitha, A review on plasmonic metal-TiO₂ composite for generation, trapping, storing and dynamic vectorial transfer of photogenerated electrons across the Schottky junction in a photocatalytic system, *Appl. Surf. Sci.* 360 (2016) 601–622.
- [40] A.A. Ismail, D.W. Bahnemann, S.A. Al-Sayari, Synthesis and photocatalytic properties of nanocrystalline Au, Pd and Pt photodeposited onto mesoporous RuO₂-TiO₂ nanocomposites, *Appl. Catal. A* 431–432 (2012) 62–68.
- [41] A. Di Paola, G. Marci, L. Palmisano, M. Schiavello, K. Uosaki, S. Ikeda, B. Ohtani, Preparation of Polycrystalline TiO₂ photocatalysts impregnated with various transition metal ions: characterization and photocatalytic activity for the degradation of 4-nitrophenol, *J. Phys. Chem. B* 106 (2002) 637–645.
- [42] E. Pulido Melián, Cristina R. López, A. Ortega Méndez, O. González Díaz, M. Nereida Suárez, J.M. Doña Rodríguez, J.A. Navío, D. Fernández Hevia, Hydrogen production using Pt-loaded TiO₂ photocatalysts, *Int. J. Hydrogen Energy* 38 (2013) 11737–11748.
- [43] M. Tahir, B. Tahir, N.A. Saidina Amin, Gold-nanoparticle-modified TiO₂ nanowires for plasmon-enhanced photocatalytic CO₂ reduction with H₂ under visible light irradiation, *Appl. Surf. Sci.* 356 (2015) 1289–1299.
- [44] J. Radnik, C. Mohr, P. Claus, On the origin of binding energy shifts of core levels of supported gold nanoparticles and dependence of pretreatment and material synthesis, *Phys. Chem. Chem. Phys.* 5 (2003) 172–177.
- [45] M.A. Aramendia, V. Borau, J.C. Colmenares, A. Marinas, J.M. Marinas, J.A. Navío, F.J. Urbano, Modification of the photocatalytic activity of Pd/TiO₂ and Zn/TiO₂ systems through different oxidative and reductive calcination treatments, *Appl. Catal. B* 80 (2008) 88–97.
- [46] A.V. Vorontsov, E.N. Savinov, Jin Zhensheng, Influence of the form of photodeposited platinum on titania upon its photocatalytic activity in CO and acetone oxidation, *J. Photochem. Photobiol. A* 125 (1999) 113–117.
- [47] J.J. Murcia, J.A. Navío, M.C. Hidalgo, Insights towards the influence of Pt features on the photocatalytic activity improvement of TiO₂ by platinisation, *Appl. Catal. B* 126 (2012) 76–85.
- [48] Z.H.N. Al-Azri, W.T. Chen, A. Chan, V. Jovic, T. Ina, H. Idriss, G.I.N. Waterhouse, The roles of metal co-catalysts and reaction media in photocatalytic hydrogen production: performance evaluation of M/TiO₂ photocatalysts (M = Pd, Pt, Au) in different alcohol-water mixtures, *J. Catal.* 329 (2015) 355–367.
- [49] S.H. Kim, C.H. Jung, N. Sahu, D. Park, J.Y. Yun, H. Ha, J.Y. Park, Catalytic activity of Au/TiO₂ and Pt/TiO₂ nanocatalysts prepared with arc plasma deposition under CO oxidation, *Appl. Catal. A* 454 (2013) 53–58.
- [50] N. Kruse, S. Chenakin, XPS characterization of Au/TiO₂ catalysts: binding energy assessment and irradiation effects, *Appl. Catal. A* 391 (2011) 367–376.
- [51] M.C. Hidalgo, J.J. Murcia, J.A. Navío, G. Colón, Photodeposition of gold on titanium dioxide for photocatalytic phenol oxidation, *Appl. Catal. A* 397 (2011) 112–120.
- [52] S. Chin, E. Park, M. Kim, J. Jeong, G.N. Bae, J. Jurng, Preparation of TiO₂ ultrafine nanopowder with large surface area and its photocatalytic activity for gaseous nitrogen oxides, *Powder Technol.* 206 (2011) 306–311.
- [53] J. Jeong, J. Jurng, S. Jin, Y. Kim, Optimization of the removal efficiency of nitrogen oxides in the air using a low-pressure Hg lamp, *J. Photochem. Photobiol. A* 197 (2008) 50–54.
- [54] M. Sleiman, P. Conchon, C. Ferronato, J.M. Chovelon, Photocatalytic oxidation of toluene at indoor air levels (ppbv): Towards a better assessment of conversion, reaction intermediates and mineralization, *Appl. Catal. B* 86 (2009) 159–165.
- [55] A. Golabiewska, A. Malankowska, M. Jarek, W. Lisowski, G. Nowaczyk, S. Jurga, A. Zaleska-Medyńska, The effect of gold shape and size on the properties and

- visible light-induced photoactivity of Au-TiO₂, *Appl. Catal. B* 196 (2016) 27–40.
- [56] V. Subramanian, E.E. Wolf, P.V. Kamat, *Catalysis with TiO₂/gold nanocomposites. Effect of metal particle size on the Fermi level equilibration*, *J. Am. Chem. Soc.* 126 (2004) 4943–4950.
- [57] E. Kowalska, S. Rau, B. Ohtani, *Plasmonic titania photocatalysts active under UV and visible-light irradiation: influence of gold amount, size, and shape*, *J. Nanotechnol.* 212 (2012) 1–11.
- [58] A.M. Dalcin Fornari, M. Brambilla de Araujo, C. Bergamin Duarte, G. Machado, S.R. Teixeira, D.E. Weibel, *Photocatalytic reforming of aqueous formaldehyde with hydrogen generation over TiO₂ nanotubes loaded with Pt or Au nanoparticles*, *Int. J. Hydrogen Energy* 41 (2016) 11599–11607.
- [59] J. Low, B. Cheng, J. Yu, *Surface modification and enhanced photocatalytic CO₂ reduction performance of TiO₂: a review*, *Appl. Surf. Sci.* 392 (2017) 658–686.
- [60] Y. Ishibai, J. Sato, S. Akita, T. Nishikawa, S. Miyagishi, *Photocatalytic oxidation of NO_x by Pt-modified TiO₂ under visible light irradiation*, *J. Photochem. Photobiol. A* 188 (2007) 106–111.
- [61] J. Uddin, J.E. Peralta, G.E. Scuseria, *Density functional theory study of bulk platinum monoxide*, *Phys. Rev. B* 71 (2005) 155112.
- [62] A. Meng, J. Zhang, D. Xu, B. Cheng, J. Yu, *Enhanced photocatalytic H₂-production activity of anatase TiO₂ nanosheet by selectively depositing dual-cocatalysts on {101} and {001} facets*, *Appl. Catal. B* 198 (2016) 286–294.
- [63] B.K. Min, J.E. Heo, N.K. Youn, O.S. Joo, H. Lee, J.H. Kim, H.S. Kim, *Tuning of the photocatalytic 1,4-dioxane degradation with surface plasmon resonance of gold nanoparticles on titania*, *Catal. Commun.* 10 (2009) 712–715.